

Cluster virial expansion and electron-hydrogen molecule scattering

Y. A. Omarbakiyeva,^{1,2,*} H. Reinholz,¹ and G. Röpke¹

¹*Institute of Physics, University of Rostock, D-18051, Rostock, Germany*

²*International IT University, 050040, Almaty, Kazakhstan*

(Dated: July 24, 2014)

The equation of state of partially ionized hydrogen plasma is considered with special focus on the contribution of $e - \text{H}_2$ interaction. Within a cluster virial expansion, the Beth-Uhlenbeck formula is applied to infer the contribution of bound and scattering states to the temperature dependent second virial coefficient. The scattering states are calculated using the phase expansion method with the polarization interaction model that incorporates experimental data for the $e - \text{H}_2$ scattering cross section. We present results for the scattering phase shifts, differential scattering cross sections, the second virial coefficient due to $e - \text{H}_2$ interaction. The influence of this interaction on the composition of the partially ionized hydrogen plasma is confined to the parameter range where both the H_2 and the free electron components are abundant.

PACS numbers: 52.25.Kn, 52.20.Hv

I. INTRODUCTION

The equation of state describing fundamental characteristics of matter attracts significant attention of researchers from multiple disciplines. For instance, the calculation of thermodynamic properties of plasmas in the warm dense matter region is necessary to solve problems of high energy density physics [1] and to model the planetary and stellar interiors [2, 3]. Correlations and bound state formation are of relevance since simple treatment of plasma using perturbation methods is not possible in this region. In particular, non-ideal contributions are involved due to the interaction between charged and neutral particles, which can be treated either within the chemical or the physical picture.

In the chemical picture, the plasma is assumed to consist of well-defined, reacting particles - electrons, ions, atoms and molecules. Interactions are described via effective short-range potentials for neutral particles and long range potential between charged particles. The thermodynamical characteristics of non-ideal plasma can be represented by the free energy, which is calculated on the basis of different pseudopotential models for certain pair interaction. Usually, the non-ideal part of the free energy consists of the contributions for Coulomb interaction (electron-electron, ion-ion, ion-electron), polarization interactions between charged and neutral particles and short-range interactions between neutrals. This model has been successfully applied [4] to investigate properties of partially ionized plasmas. Nevertheless it should be systematically studied within quantum-statistical methods to avoid inconsistencies such as double counting effects.

In the physical model, the fundamental structural elements are the electrons and protons with Coulomb interaction, and the composite particles, atoms, molecules

and other heavier components are obtained from few-body wave equations. The latter are assumed to consist of fundamental particles and their properties should be determined by solving the corresponding Schrödinger equation. Within the physical picture, virial expansions (with respect to density or fugacity) can be evaluated. In the density virial expansion, the second virial coefficient is determined by pair interactions. Interactions of electrons with the neutral composite particles appear in higher orders (third virial coefficient etc.). Alternatively, the contribution of neutral particles can be taken into account within a cluster virial expansion. In the fugacity expansion, formation of bound states (clusters) are consistently included. For instance, in the low density limit two-particle bound states are stable. Therefore, it is possible to consider the bound states as new particles. We switch from the physical picture to the chemical picture what means the partial summation of ladder diagrams that describes the formation of bound states with a Green function approach. The three particle interaction in the physical picture will be considered as effective two particle interaction in the chemical picture after inclusion of cluster states.

The cluster virial expansion has been described in details in a previous paper [5]. The electron-atom interaction was studied from a microscopic point of view. Different pseudopotentials were compared and empirical data for separable potentials were given. With the help of the Beth-Uhlenbeck formula [6] it has been shown that the second virial coefficient in the electron-atom channel is related to scattering phase shifts as well as bound states. In contrast to previous approaches, results for the second virial coefficient in the $e - \text{H}$ channel are not based on any pseudopotential models but are directly derived from measured scattering data. Simultaneously, the contribution of the bound state H^- was included. The use of experimental data as an input for the Beth-Uhlenbeck formula avoids any empirical parameters and may be considered as low-density benchmark for any equation of state. In this present work, this approach will be ex-

* yultuz.omarbakiyeva@uni-rostock.de

tended to include further components of the plasma, in particular H_2 molecules interacting with electrons.

We study partially ionized hydrogen plasma with electrons (e), ions (protons i), hydrogen atoms (H), and hydrogen molecules (H_2) as constituents starting from the chemical picture. We focus on the interaction of $e - \text{H}_2$ and its contribution to the equation of state. The influence of the molecular component is essential in dense partially ionized plasmas. The composition of hydrogen plasma has been calculated following a set of mass action laws [7]. Fig.1 presents a standard approach [7] to the composition of hydrogen plasma, exemplarily for $T = 15000$ K, with fractions $\alpha_c = Z_c n_c / n_e^{\text{tot}}$, n_c is density of species, n_e^{tot} is total electron density, Z_c is the number of electrons in the corresponding bound states. The free electron fraction is decreasing until total electron densities of 10^{23} cm^{-3} before pressure ionization sets in. The fraction of hydrogen atoms is dominating in the density region $\approx 10^{18} - 10^{24} \text{ cm}^{-3}$. At densities above 10^{21} cm^{-3} , the molecule fraction plays an essential role in physical processes. Note, that following [7] the interactions between electrons and clusters are taken into account by a hard-core model to calculate the composition in Fig.1. The use of experimental data for the interaction parts of chemical potentials can give more accurate data for the composition. In the present work, we consider partially ionized hydrogen plasmas at temperatures $T \leq 10^5$ K and densities up to 10^{22} cm^{-3} until degeneracy effects play an essential role. As a new ingredient, the contribution of scattering states is considered. We apply the cluster virial expansion approach to study the contribution of the electron-molecule interaction to thermodynamical properties. The present work is organized as follows: In Section II, we briefly review the cluster-virial expansion and the Beth-Uhlenbeck formula for the second virial coefficient. Section III contains the calculation of the scattering phase shifts for the electron-molecule system, both via experimental differential cross sections and phase shifts from appropriate pseudopotentials. In Section IV, the phase shifts are used to calculate the corresponding second virial coefficient. Results for the $\text{H}_2 - e$ second virial coefficient are given for different temperatures, and consequences for the composition are considered. Conclusions are drawn in Section V.

II. CLUSTER VIRIAL EXPANSION AND BETH-UHLENBECK FORMULA

The cluster virial expansion for the equation of state [8] can be written as function of fugacities, $z_c = e^{\beta(\mu_c - E_c^{(0)})}$,

$$\beta p = \sum_c \frac{2s_c + 1}{\Lambda_c^3} (z_c + \sum_d z_c z_d \tilde{b}_{cd} + \dots), \quad (1)$$

where c denotes species ($c = e, i, \text{H}, \text{H}_2$), s_c - spin, μ_c - chemical potential, $E_c^{(0)}$ - binding energy for isolated cluster species, $\Lambda_c = (2\pi\hbar^2/k_B T m_c)^{1/2}$ - the thermal

wavelength of species c . The first term is the ideal part of the pressure. The contribution of the Coloumb interaction between charge particles and the interaction with neutrals must be treated differently. For the Coloumb interactions ($e - e$, $e - i$, $i - i$), the non-ideal contributions of the equation of state have been intensively investigated, for a review see Ref. [9]. For the interaction with neutrals the dimensionless second virial coefficient \tilde{b}_{cd} is determined by the respective interactions of $e - \text{H}$, $i - \text{H}$, $\text{H} - \text{H}$, $e - \text{H}_2$, $i - \text{H}_2$, $\text{H}_2 - \text{H}_2$, $\text{H} - \text{H}_2$ pairs. In particular, \tilde{b}_{HH} was calculated in Refs. [10] and $\tilde{b}_{e\text{H}}$ was studied in Ref. [5].

An exact quantum mechanical expression for the second virial coefficient was given by Beth and Uhlenbeck [8]:

$$\tilde{b}_{cd} = \sum_{\ell} (2\ell + 1) \sum_n (e^{-\beta E_{cd}^{n\ell}} - 1) + \sum_{\ell=0}^{\infty} (2\ell + 1) \frac{\beta}{\pi} \int_0^{\infty} e^{-\beta E} \eta_{\ell}^{cd}(E) dE, \quad (2)$$

where ℓ is orbital momentum, $\eta_{\ell}^{cd}(E)$ is the scattering phase shift, E is the energy of incident particles, $E_c^{n\ell}$ is binding energy of the state with quantum numbers $n\ell$. The first term is the bound part $\tilde{b}_{cd}^{\text{bound}}$ and the second is the scattering part $\tilde{b}_{cd}^{\text{sc}}$.

In this paper we focus on the second virial coefficient for $e - \text{H}_2$. We calculate the scattering part of the second virial coefficient $\tilde{b}_{\text{H}_2 e}$ due to electron and hydrogen molecule interaction. The bound part includes a new component H_2^- in the system. The calculation of the bound part requires the binding energy of the negative hydrogen molecule, which was taken from the literature [11]. Note that alternatively to Eq.(2), the bound state H_2^- can be considered as a new species c in calculating thermodynamic properties.

III. SCATTERING DATA

Scattering phase shifts data for $e - \text{H}_2$ can be employed to calculate the second virial coefficient $\tilde{b}_{\text{H}_2 e}$ using the Beth-Uhlenbeck formula (2). Due to internal degrees of freedom of the H_2 molecule, the $e - \text{H}_2$ scattering problem is more complex compared to the $e - \text{H}$ system. In addition to electronic excitation and ionization, other processes at energies below the ionization limit $E_i = 124417.49 \text{ cm}^{-1} \approx 15.42 \text{ eV}$ [12] have to be considered. It is clear that the total cross section Q_{T} includes all these processes:

$$Q_{\text{T}} = Q_{\text{elas}} + Q_{\text{att}} + Q_{\text{diss}} + \sum Q_{\text{excit}}, \quad (3)$$

where cross sections for elastic scattering is Q_{elas} , for dissociative attachment is Q_{att} , for impact dissociation is Q_{diss} . $\sum Q_{\text{excit}}$ is the sum of all excitation cross sections of rotational, vibrational, and electronic states. Table I shows the contribution of those transitions, which were

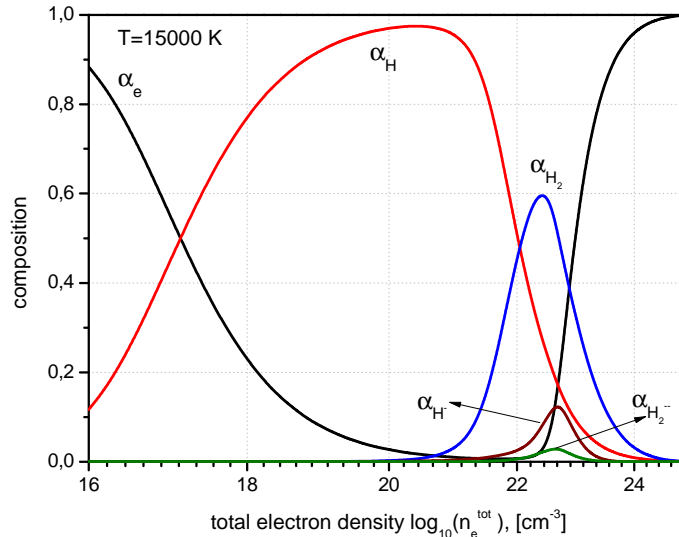


FIG. 1. (Color online) The composition of hydrogen plasmas for $T = 15000$ K

TABLE I. Contribution of various transitions to total $e - \text{H}_2$ scattering cross sections [a_B^2] at different impact energies

Transition \ energy [eV]	7	10	13.6	20	45	60	81.6
A. Total scattering [14]	42.1	33.7	26.9	20.0			
B. Electronic excitation [13]	0.0	0.73	3.27	5.23			
C. A minus B	42.1	33.0	23.6	14.8			
D. Elastic scattering [13]	41.5	32.6	23.4	14.7	7.86	5.97	4.44
E. Vibrational excitation [13]	0.60	0.35	0.11	0.05	0.05	0.03	0.03

estimated in Ref.[13]. The rotational excitation is not given. However, this channel is mixed into elastic and vibrational excitation transitions. As can be seen in Table I, the electronic excitation channel is closed until 7 eV. The vibrational transition is about 1.4% at 7 eV of total cross section and it is decreasing with increasing incident energy. Up to 10 eV the total cross section is dominated by elastic contributions. This statement is further verified by considering the collision cross sections, see Figure 2. The total cross section Q_T is obtained from beam measurements and was determined as recommended value in Ref. [15]. The rotational excitation channel is already open at $44 \cdot 10^{-3}$ eV for the lowest rotational state ($J = 0 \rightarrow 2$). The vibrational channel sets in at 0.516 eV, the electronic excitation channel at 7 eV. The contributions of electronic, rotational, and vibrational excitations to the total cross section below 10 eV are not more than 1.04%, 10%, and 2.89%, respectively. Note that Q_{rot} is determined from theoretical calculations [16]. According to these estimations, the $e - \text{H}_2$ scattering process below 10 eV is determined with sufficient accuracy by the elastic contribution only.

A. $e - \text{H}_2$ scattering theory

Various theoretical methods were developed to solve the Schrödinger equation for $e - \text{H}_2$ scattering process. The T-matrix expansion method, the Schwinger variational method, the R-matrix method are so called basis-set expansion methods applied for electron-molecule system (see the detailed review of theoretical methods in Ref. [17]). An alternative approach is an one-particle picture for the description of the elastic scattering process in fixed-nuclei (Born-Oppenheimer) limit [17]. Molecules are fixed in position and the Schrödinger equation is solved for the electrons in the static electric potential arising due to the molecular configuration.

In this paper, we use the simplest approximation to solve the scattering problem of electron-hydrogen molecule system. We assume that molecules are fixed in space and it is not rotating and not vibrating. In this case, the interaction between an electron and a molecule is treated similar to that of an electron-atom system. That means the electron is scattered by a optical potential V

$$H_{\text{eff}} = T_e + V, \quad (4)$$

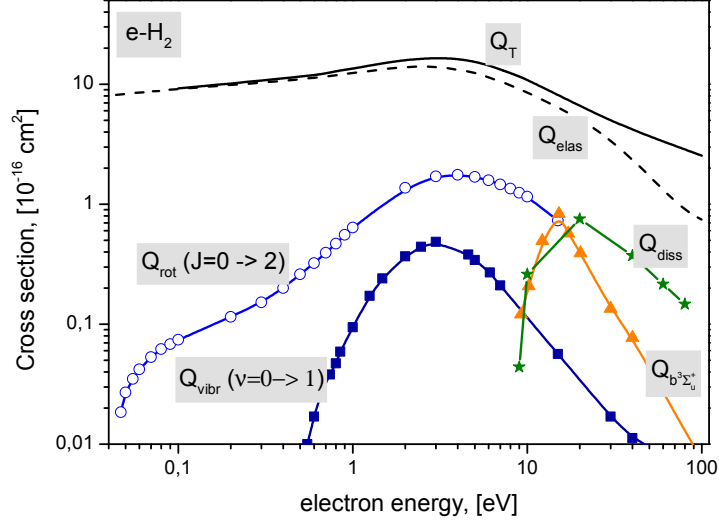


FIG. 2. (Color online) Cross section for $e\text{-H}_2$ collision. Adapted from Ref. [15]

and we use the phase function method [18, 19] to solve the Schrödinger equation.

The phase function equation or so called Calogero equation for the scattering phase shift η_ℓ is

$$\frac{d\eta_\ell^{cd}(k, r)}{dr} = -\frac{1}{k}U(r)[\cos\eta_\ell^{cd}(k, r)J_\ell(k, r) - \sin\eta_\ell^{cd}(k, r)n_\ell(k, r)]^2 \quad (5)$$

(see more details in Ref. [20]). The Calogero equation has an initial condition $\eta_\ell^{cd}(k, 0) = 0$, where k is the wave number, ℓ are orbital quantum numbers, $J_\ell(k, r)$ and $n_\ell(k, r)$ are the Riccati-Bessel functions, $U(r) = \frac{2m_{cd}}{\hbar^2}V(r)$, $V(r)$ is the interaction potential. The energy-dependent scattering phase shifts $\eta_\ell^{cd}(k)$ are determined as $\eta_\ell^{cd}(k) = \lim_{r \rightarrow \infty} \eta_\ell^{cd}(k, r)$.

B. Interaction potential

As we mentioned above, the accurate calculation of the scattering problem requires an adequate approximation of the optical potential. It is a full projectile-target (electron-molecule) interaction potential which consists of static, exchange and polarization contributions. The static potential is given by the electrostatic interaction between the projectile and the constituent particles of the target [16]. The exchange effect is important at low energies, it occurs due to indistinguishability of the projectile and target electrons. The polarization potential describes induced distortions of the target by the impact electron. Since the goal is to consider a collision process in plasma, the last effect (polarization) is particularly important for the description of plasma properties. Collisions of electrons on molecules in plasmas with not too

high densities occurs at large distances. The polarization potential for the electron-atom interaction has the asymptotic behavior $\alpha/2r^4$ (at large distances) with the polarizability α of the atom. Since this potential is diverging at small distances, the Buckingham potential was suggested for $e-a$ interaction [21]:

$$V_{ea} = -\frac{\alpha}{2(r^2 + r_0^2)^2}, \quad (6)$$

where r_0 is a cut-off radius. For hydrogen atoms $\alpha = 4.5 a_B^3$ and $r_0 = 1.456 a_B$ [22]. If we consider interaction of electrons with diatomic molecules, the polarization model is modified [16, 17]:

$$V_{eH_2}(r) = \left(-\frac{\alpha_0}{2r^4} - \frac{\alpha_2}{2r^4} P_2(\cos\theta_p) \right) \times \left(1 - \exp(r/r_0)^6 \right), \quad (7)$$

where α_0 and α_2 are polarizabilities parallel and perpendicular to the internuclear axis \vec{e}_R , respectively. $P_2(\cos\theta_p)$ is the Legendre polynomial. θ_p is the angle between the direction of the incident electron and the z -axis. This potential describes the interaction of molecule positioned at the origin and the z -axis coincides with \vec{e}_R . For H_2 (internuclear distance $R = 1.4 a_B$), we use the experimental data of polarizabilities $\alpha_0 = 5.4265 a_B^3$, $\alpha_2 = 1.3567 a_B^3$ [16].

C. Phase shifts

The solution of the Calogero equation is used to obtain the scattering phase shifts. The results for different orbital momenta on the basis of the polarization model

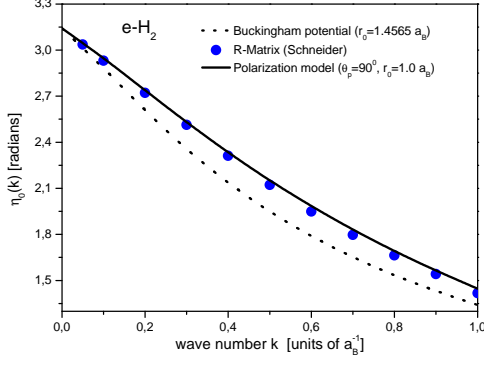


FIG. 3. (Color online) s-wave scattering phase shifts for $e - \text{H}_2$. R - matrix data [23] is compared with the results of the present calculation on the basis of the polarization models (7) and (6)

(7) are shown in the Figures 3, 4 and 5. We consider the phase shifts results in Fig.3. At $k = 0$ the s-wave scattering phase shifts $\eta_0(0)$ tends to the value of π . According to the Levinson theorem [24] $\eta(0) = n\pi$ (where n is the number of bound states), it corresponds to one bound state. In our case it is the negative hydrogen molecule. H_2^- is a metastable state, that appears in reactions like dissociative attachment ($\text{H}_2 + e \rightarrow \text{H}_2^- \rightarrow \text{H} + \text{H}^-$) and associative attachment ($\text{H} + \text{H}^- \rightarrow \text{H}_2^- \rightarrow \text{H}_2 + e$). The stability of this state is discussed in the literature. Recently, the lifetime of this metastable state was measured as $5 - 8 \mu\text{s}$ [25]. The theoretical value of electron affinity (or binding energy) for the bound state H_2^- is $2.08 \cdot 10^{-2}$ eV/atom corresponding to 2 kJ/mole [11]. This value has been taken to calculate the bound part of the second virial coefficient in the Beth-Uhlenbeck formula (2).

The phase shifts data for the s-channel are compared with the R-matrix data of Ref. [23]. As one can see, the present results for the polarization model (7) have good agreement with Schneider's data. The parameter values of the polarization potential (7) r_0 and θ_p are fit to get a good agreement in phase shifts with theoretical data. The cut-off radius in this calculation is taken as $r_0 = 1.0 a_B$, and $\theta_p = 90^\circ$. Note, that no direct measurements of the phase shifts can be found in literature, only scattering cross section data.

In Figures 4 and 5 the scattering phase shifts for $\ell = 1, 2$ are presented using the same parameters for r_0 and θ_p as for s-wave. Both phase shifts are zero at zero incident energy of the electron, since no bound states exist for these scattering channels. The d-wave results are very small in comparison with the s channel at low energy limit. In general, to calculate the second virial coefficients the phase shifts for $\ell < 3$ are enough to obtain accurate results. The comparison of p- and d- waves with Schneider's data [23] shows deviations. This can be explained by the different methods we used and neglec-

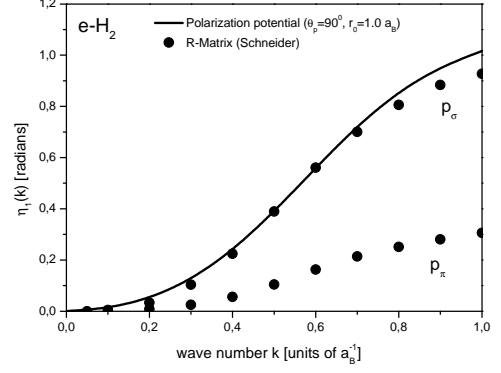


FIG. 4. p-wave scattering phase shifts for $e - \text{H}_2$. R - matrix data [23] is compared with the results of the present calculation on the basis of the polarization model (7)

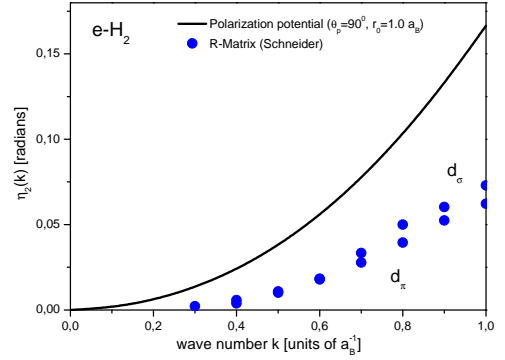


FIG. 5. (Color online) d-wave scattering phase shifts for $e - \text{H}_2$. R - matrix data [23] is compared with the results of the present calculation on the basis of the polarization model (7)

tion of symmetry effects in our approach. In the present calculation, a molecule without structure is considered, so the comparison of data with other theoretical works in σ and π orbitals is not possible. The only confirmation of this studies can be the comparison of calculated differential cross section with experimental data.

D. Elastic differential cross section

Experimental data for the electron-molecule collisions were collected by Trajmar [26], Brunger [27] and Itikawa [15]. As was discussed above, rotational excitation channels are already open at a very low energy; for instance, the lowest rotational state energy ($J = 0 \rightarrow 2$) is $44.13 \cdot 10^{-3}$ eV. Therefore, the experimental data for elastic differential cross section include rotational excitations and are rotationally summed. Only in the experiment by Linder and Schmidt [28], elastic scattering

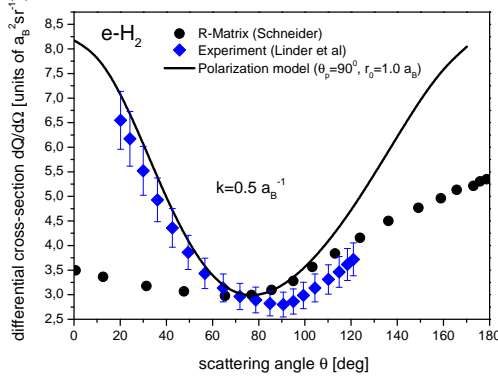


FIG. 6. (Color online) Differential cross sections for $e - \text{H}_2$ at wave number $k = 0.5 a_B^{-1}$. Solid line shows calculation with the polarization model (7); square line is experimental data Ref.[28]; triangle line is theoretical data Ref.[23]

was separated from rotational excitation. So, the data of Linder and Schmidt were taken to compare this studies' results for differential cross sections. Also recent experimental data from Muse et al. [29] are taken to perform the comparison of differential cross sections.

Using the obtained phase shifts, the differential cross sections can be calculated by the following formula:

$$\frac{dQ(k, \theta)}{d\Omega} = \left| \frac{1}{2ik} \sum_{\ell} (2\ell + 1) [e^{2i\eta_{\ell}^c(k)} - 1] P_{\ell}(\cos \theta) \right|^2, \quad (8)$$

where θ is the scattering angle (do not confuse with θ_p). In our calculation we include the orbital momentum until $\ell = 5$. The dependence of the differential cross section on scattering angle is shown in Figs. 6, 7, 8 and 9 for different incident energies of the electron. In Fig. 6 the results of the polarization model (7) is compared with R-matrix data of Schneider [23] and experimental data [28] at $k = 0.5 a_B^{-1}$. Our results describe better the collision process at small scattering angles, whereas the R-matrix data works only at middle angles. The comparison of our results with experimental data [28, 29] at other energies shows a good agreement almost at all scattering angles. With increasing incident energy, slight deviation between experiment and our calculation is observed. It can be explained by an increasing contribution of rotational excitations, which is not included in our calculation. In Fig.9 also the differential cross section for electron and atom scattering is presented. The atomic cross section, calculated using the Buckingham potential (6), is smaller than the molecular cross section almost by a factor of 2. Although we use a simple approximation to describe the scattering process between electron and hydrogen molecule, our results are reliable which was shown by comparison with experimental data.

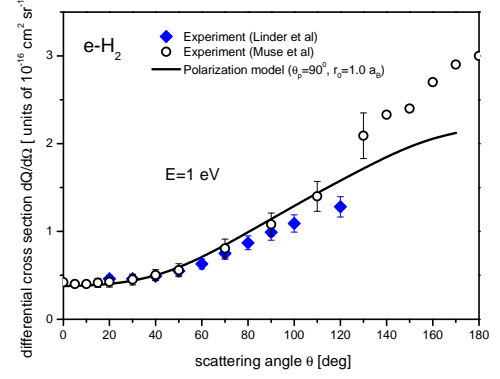


FIG. 7. (Color online) Differential cross sections for $e - \text{H}_2$ at incident energies 1 eV. Solid line presents calculation with the polarization model (7); square line is experimental data Ref.[28]; circle - experimental data Ref. [29]

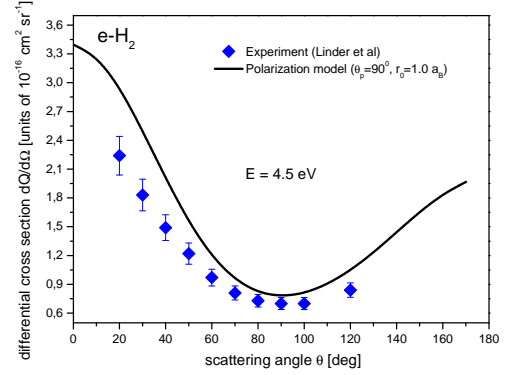


FIG. 8. (Color online) Differential cross sections for $e - \text{H}_2$ at incident energies 4.5 eV. Solid line presents calculation with the polarization model (7); square line is experimental data Ref.[28]

IV. RESULTS AND DISCUSSION

A. Second virial coefficient for $e - \text{H}_2$ interaction

The data of scattering phase shifts shown in the Figures 3, 4 and 5 which are based on experimental data, will be used for calculations of the second virial coefficient using the Beth-Uhlenbeck formula (2). The phase shifts are obtained using the polarization model Eq. (7). Table II shows results for the normalized second virial coefficients $\tilde{b}_{\text{H}_2e}^{\text{sc}}$ and $\tilde{b}_{\text{H}_2e}^{\text{bound}}$ for the scattering and the bound parts, respectively. The second, third and fourth columns of the table present data for the contribution of s, p, and d-waves to the scattering part of the second virial coefficient, respectively. Higher order contributions are small and negligible for the temperature range considered here. The $\tilde{b}_{\text{H}_2e}^{\text{sc}}$ for higher orbital momenta is weaker

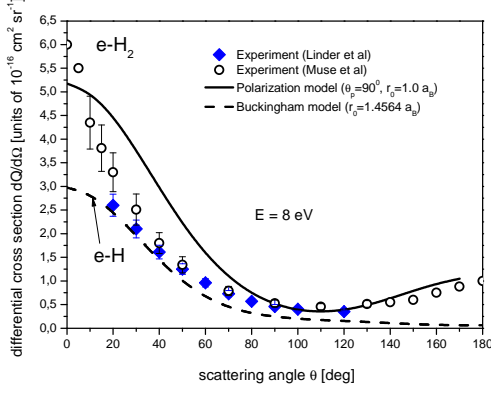


FIG. 9. (Color online) Differential cross sections for $e - \text{H}_2$ at incident energies 8 eV. Solid line presents calculation with polarization model (7); square line is experimental data Ref.[28]; circle - experimental data Ref. [29]; dashed line - present calculation with the polarization model (6)

than for the s-wave. With increasing temperature, the scattering part of the second virial coefficient for the s-wave decreases weakly, but the results for the other two channels increase. This occurs due to the difference in behaviour of phase shifts, see Figures 3, 4 and 5. The sixth column shows the bound part (H_2^-) of the second virial coefficient. The bound part is strongly depending on temperature. At low temperatures bound particles (clusters) are important. The full second virial coefficient is presented in the last column. The dependence of the full second virial coefficient on temperature is determined by the scattering part. Data from Table II can be used to study thermodynamical properties of the system. Note, that the second virial coefficients do not depend on the density of the plasma. The density dependence is included in the virial expansions for thermodynamical functions, see for instance the pressure, Eq.(1).

B. Ionization Equilibrium

The interaction between electrons and neutral clusters can play an essential role for the plasma composition. In a system with charged particles, hydrogen atoms and hydrogen molecules, the following chemical reactions are possible: $e + i \rightleftharpoons \text{H}$, $\text{H} + \text{H} \rightleftharpoons \text{H}_2$, $e + \text{H} \rightleftharpoons \text{H}^-$ and $e + \text{H}_2 \rightleftharpoons \text{H}_2^-$. Each reaction corresponds to a chemical equilibrium with respect to the chemical potentials, respectively:

$$\begin{aligned} \mu_e + \mu_i &= \mu_{\text{H}}, \\ \mu_{\text{H}} + \mu_{\text{H}} &= \mu_{\text{H}_2}, \\ \mu_e + \mu_{\text{H}} &= \mu_{\text{H}^-}, \\ \mu_e + \mu_{\text{H}_2} &= \mu_{\text{H}_2^-}. \end{aligned} \quad (9)$$

Note that the clusters H^- and H_2^- are included now as components in the chemical picture. Alternatively,

the contribution of these bound states can also be obtained consistently from the Beth-Uhlenbeck formula (2) as bound state contribution. Further possible cluster states are not considered in this work, in particular the H_2^+ bound state will be obtained in the $\text{H} - i$ interaction channel.

In non-ideal plasma the chemical potential can be divided into ideal and non-ideal parts. For instance, for the chemical potential, the following expression defines the virial coefficients [8]

$$\mu_c = \mu_c^{\text{id}} - k_B T \left(2 \sum_d n_d b_{cd} + 3 \sum_{de} n_d n_e b_{cde} + \dots \right), \quad (10)$$

where b_{cd} is the second virial coefficient. There is a connection between the dimensionless second virial coefficient \tilde{b}_{cd} (see Eq.(1)) and b_{cd} : $\tilde{b}_{cd} = b_{cd} g_d / \Lambda_d^3$, where g_d is the spin degeneracy factor. The first term of Eq.(10) $\mu_c^{\text{id}} = k_B T \ln \left(\frac{n_c \Lambda_c^3}{g_c} \right) + E_c^{(0)}$ is the ideal part of the chemical potential with binding energy $E_c^{(0)}$ of isolated clusters (H , H_2 , H^- , H_2^-). The non-ideal parts $\Delta \mu_{cd}$ are defined by the second virial coefficients b_{cd} , similar further terms $\Delta \mu_{cde}$ etc. of Eq.(10). The virial expansion is diverging for Coulomb interactions (for $e - e$, $i - i$, $e - i$ contributions). Therefore we consider screening interaction and take as an approximation for protons the classical Debye shift $\Delta_i = -\kappa e^2 / 2$ with the inverse screening length $\kappa^2 = \left(\frac{4\pi n_i e^2}{k_B T} \right)$. For electrons we use the Padé formulae [7], which can be used at any plasma degeneracy

$$\Delta_e = \frac{\mu_D - \frac{1}{2}(\pi\beta)^{-1/2}\bar{n} + 8\bar{n}^2\mu_{\text{GB}}}{1 + 8\ln[1 + \frac{1}{16\sqrt{2}}(\pi\beta)^{1/4}\bar{n}^{1/2}] + 8\bar{n}^2}, \quad (11)$$

where $\bar{n} = n_e \Lambda_e^3$, $\mu_D = -(\pi\beta)^{-1/4}\bar{n}^{1/2}$ is the chemical potential in low-density limit (Debye limiting law), and $\mu_{\text{GB}} = -\frac{1.2217}{r_s} - 0.08883 \ln[1 + \frac{6.2208}{r_s^{0.7}}]$ is the Gell-Mann-Brueckner approximation for the highly degenerate region (in [Ryd]), $r_s = (3/(4\pi n_e))^{1/3}/a_B$ is the Brueckner parameter.

Finally, using the equations (9) and (10) the system of equations can be solved to derive the composition of the plasma with components $e, i, \text{H}, \text{H}_2, \text{H}^-, \text{H}_2^-$

$$\begin{aligned} \frac{n_{\text{H}}}{n_e n_i} &= \Lambda_e^3 \exp(-\beta E_0) \exp \left[\beta(\Delta_e + \Delta_i - \Delta \mu_{\text{HH}}^{\text{sc}} + \Delta \mu_{e\text{H}}^{\text{sc}} + \Delta \mu_{e\text{H}_2}^{\text{sc}}) \right], \\ \frac{n_{\text{H}_2}}{n_{\text{H}}^2} &= b_{\text{HH}}^{\text{bound}} \exp \left[\beta(2\Delta \mu_{\text{HH}}^{\text{sc}} - \Delta \mu_{\text{H}_2\text{H}_2}^{\text{sc}}) \right], \\ \frac{n_{\text{H}^-}}{n_e n_{\text{H}}} &= b_{\text{He}}^{\text{bound}} \exp \left[\beta(\Delta_e + \Delta \mu_{\text{HH}}^{\text{sc}}) \right], \\ \frac{n_{\text{H}_2^-}}{n_e n_{\text{H}_2}} &= b_{\text{H}_2e}^{\text{bound}} \exp \left[\beta(\Delta_e + \Delta \mu_{\text{H}_2\text{H}_2}^{\text{sc}}) \right], \\ n_e^{\text{tot}} &= n_e + n_{\text{H}} + 2n_{\text{H}_2} + 2n_{\text{H}^-} + 3n_{\text{H}_2^-}, \end{aligned} \quad (12)$$

where $E_0 = 13.6$ eV is the ground state energy of hydrogen. The bound parts of the second virial coefficients

TABLE II. Scattering and bound part of the second cluster virial coefficient \tilde{b}_{H_2e} for different temperatures.

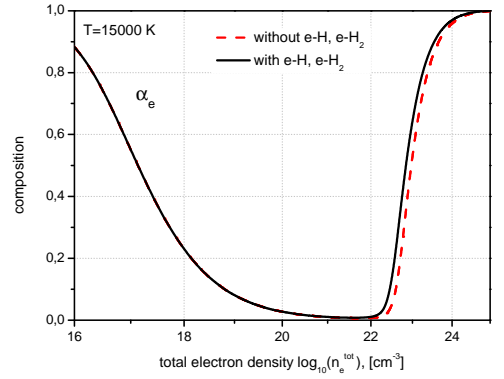
T , [K]	$\tilde{b}_{\text{H}_2e}^{\text{sc}}$, s-wave	$\tilde{b}_{\text{H}_2e}^{\text{sc}}$, p-wave	$\tilde{b}_{\text{H}_2e}^{\text{sc}}$, d-wave	$\tilde{b}_{\text{H}_2e}^{\text{sc}}$, full	$\tilde{b}_{\text{H}_2e}^{\text{bound}}$	\tilde{b}_{H_2e} , full
5000	0.9308	0.0179	0.0034	0.9522	0.0494	1.0015
7000	0.9173	0.0260	0.0049	0.9499	0.0350	0.9832
8000	0.9113	0.0301	0.0056	0.9482	0.0306	0.9776
9000	0.9056	0.0343	0.0064	0.9464	0.0271	0.9734
10000	0.9002	0.0386	0.0071	0.9460	0.0244	0.9703
11000	0.8951	0.0429	0.0079	0.9460	0.0222	0.9682
12000	0.8903	0.0473	0.0086	0.9462	0.0203	0.9665
13000	0.8856	0.0517	0.0094	0.9468	0.0187	0.9656
14000	0.8813	0.0562	0.0101	0.9476	0.0173	0.9649
15000	0.8770	0.0607	0.0108	0.9485	0.0162	0.9647
20000	0.8576	0.0836	0.0146	0.9560	0.0121	0.9681

are $b_{\text{HH}}^{\text{bound}}$, $b_{\text{He}}^{\text{bound}}$ and $b_{\text{H}_2e}^{\text{bound}}$. The dissociation energy of hydrogen molecule $D_0 = 4.75$ eV, the vibrational constant $h\nu/k_B = 6338.2$ K [30] and the rotational constant $B = 87.58$ K [30] are included in the bound part of the second virial coefficient

$$b_{\text{HH}}^{\text{bound}} = \frac{1}{\sqrt{2}} \Lambda_{\text{H}}^3 \left(\frac{T}{B} \right) \frac{1}{1 - \exp(-h\nu/k_B T)} \exp(\beta D_0). \quad (13)$$

$\Delta\mu_{cd}^{\text{sc}} = -2n_d b_{cd}^{\text{sc}}/\beta$ is scattering part of the non-ideal part of chemical potential for species c , d . The second virial coefficient for $\text{H}_2 - \text{H}_2$ interaction is treated using hard-core model $b_{\text{H}_2\text{H}_2} = \frac{2\pi}{3} d_{\text{H}_2}^3(T)$. The diameter of hydrogen molecule d_{H_2} and $b_{\text{HH}}^{\text{sc}}$ are taken from Ref. [7]. Data for the second virial coefficient b_{He} are taken from the previous work [5]. Other second virial coefficient b_{H_2e} are taken from our calculation, see Table II.

We focus on the influence of these two interactions ($e-\text{H}$ and $e-\text{H}_2$) on the ionization equilibrium. Solution of the coupled equations (12) for temperature $T = 15000$ K are shown in the Figs. 10 and 11 in terms of fractions $\alpha_e = n_e/n_e^{\text{tot}}$, $\alpha_{\text{H}} = n_{\text{H}}/n_e^{\text{tot}}$, $\alpha_{\text{H}_2} = 2n_{\text{H}_2}/n_e^{\text{tot}}$, $\alpha_{\text{H}^-} = 2n_{\text{H}^-}/n_e^{\text{tot}}$ and $\alpha_{\text{H}_2^-} = 3n_{\text{H}_2^-}/n_e^{\text{tot}}$. Selected data are also given in Tables III and IV. Figure 10 shows the results for the electron fraction with and without interaction terms $\Delta\mu_{e\text{H}}^{\text{sc}}$ and $\Delta\mu_{e\text{H}_2}^{\text{sc}}$. Corrections are observed only at higher densities. The inclusion of these additional interactions leads to an increase of the electron fraction at the same total electron density. Figure 11 shows the comparison of all fractions with and without the interaction terms. Corrections due to the additional interaction considered here can be seen at total electron densities $10^{21} - 10^{22} \text{ cm}^{-3}$. At this density range, the fractions α_{H} , α_{H_2} and α_e are relatively large and the interaction between electrons and atoms as well as molecules gives a significant contribution to the composition.

FIG. 10. (Color online) Fraction α_e with and without interaction terms at $T = 15000$ KTABLE III. Fractions for e , H , H_2 , H^- and H_2^- with interaction terms for $e - \text{H}$ and $e - \text{H}_2$ at $T = 15000$ K

n_e^{tot} , [cm^{-3}]	α_e	α_{H}	α_{H_2}	α_{H^-}	$\alpha_{\text{H}_2^-}$
10^{16}	0.883	0.117	$1.09 \cdot 10^{-8}$	$4.15 \cdot 10^{-7}$	$1.32 \cdot 10^{-13}$
10^{18}	0.230	0.770	$4.75 \cdot 10^{-5}$	$6.94 \cdot 10^{-5}$	$1.46 \cdot 10^{-8}$
10^{20}	0.027	0.964	0.0077	0.000957	$2.62 \cdot 10^{-5}$
10^{21}	0.011	0.891	0.0939	0.00315	0.0011
10^{22}	0.039	0.381	0.531	0.0202	0.0292
10^{23}	0.816	0.050	0.129	0.00396	0.000204

C. Comparison with the excluded volume approach

The excluded volume concept is one of the popular simpler approximations to take the interaction of electrons with neutrals into account [31]. The fraction of volume occupied by atoms can be defined with the filling parameter $\eta = 4/3\pi r_{\text{H}}^3 n_{\text{H}}$, where r_{H} is an atomic radius.

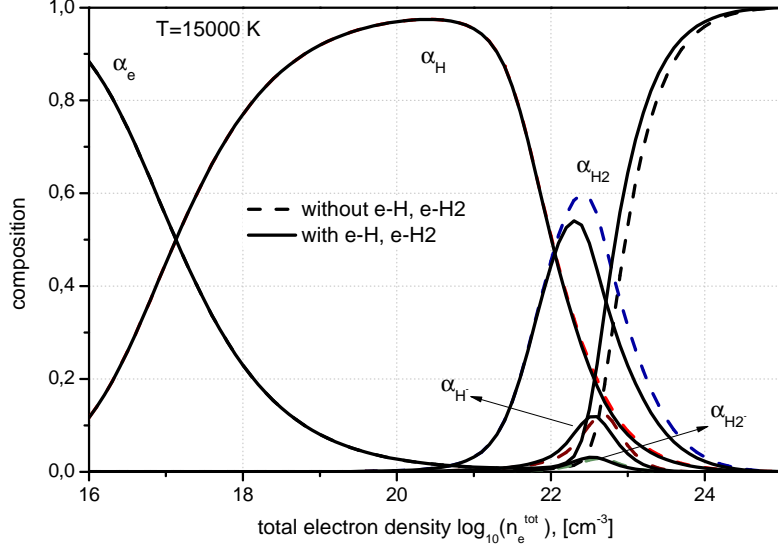


FIG. 11. (Color online) Composition for e , H , H_2 , H^- , H_2^- with and without interaction terms at $T = 15000$ K

TABLE IV. Fractions for e , H , H_2 , H^- and H_2^- without interaction terms for $e - H$ and $e - H_2$ at $T = 15000$ K

$n_e^{\text{tot}}, [\text{cm}^{-3}]$	α_e	α_H	α_{H_2}	α_{H^-}	$\alpha_{H_2^-}$
10^{16}	0.883	0.117	$1.09 \cdot 10^{-8}$	$4.15 \cdot 10^{-7}$	$1.32 \cdot 10^{-13}$
10^{18}	0.230	0.770	$4.75 \cdot 10^{-5}$	$6.94 \cdot 10^{-5}$	$1.45 \cdot 10^{-8}$
10^{20}	0.027	0.964	0.0077	0.000967	$2.59 \cdot 10^{-5}$
10^{21}	0.009	0.892	0.094	0.003	0.001
10^{22}	0.007	0.387	0.566	0.014	0.025
10^{23}	0.534	0.069	0.322	0.031	0.043

The second virial coefficient is given for a system of hard spheres as

$$b_{eH}^{\text{ex}} = -\frac{2}{3}\pi r_H^3. \quad (14)$$

The composition of partially ionized hydrogen plasma is calculated replacing b_{He}^{sc} in the previous calculations by the second virial coefficient from excluded volume concept b_{eH}^{ex} with the hard-core radius of $r_H = 1.0 a_B$. Within the considered accuracy, this leads approximately to identical results as for the calculations without electron-atom interaction, see Table IV. It indicates that the excluded volume concept with $r_H = 1.0 a_B$ makes the interaction of electrons and clusters negligible.

On the other hand, it is interesting to fit the radii of hydrogen atoms and molecules on the basis of the second virial coefficients according to Eq.(14). Using the data for b_{He} from the previous paper Ref. [5] and for b_{H_2e} from Table II, one can obtain the corresponding radii. Table V shows the results of the fit for different temperatures. The increase of temperature leads to smaller radii. High

energy of projectile electrons leads to fast collisions and closer distances. In the last two columns of the Table V, data from Ref. [7] are given. The radii are obtained by fitting of the classical virial coefficients assuming real potential for $H - H$ and $H_2 - H_2$ interactions.

Note that the mean particle distance $d_e = d_i = (3/4\pi n_e^{\text{tot}})^{1/3}$ gives a general limit of applicability of the cluster virial expansion for temperature and density parameters. At the total electron density $n_e^{\text{tot}} = 1.37 \cdot 10^{22} \text{cm}^{-3}$ the mean particle distance is $d_e = 4.90 a_B$. That means, at $T = 15000$ K the use of the second virial coefficients is possible up to this density.

V. CONCLUSIONS

The cluster virial expansion for thermodynamical functions is considered for a partially ionized plasma. Using the Beth-Uhlenbeck formula [6], the second virial coefficient in the electron-molecule ($e - H_2$) channel is related to phase shifts and possible bound states in that channel. Results for the $e - H_2$ channel are based on the polarization pseudopotential model (7) which is adapted to experimental data of scattering cross sections. A new bound state H_2^- occurs in the bound part of the Beth-Uhlenbeck formula. Alternatively, it can be considered as a new constituent within the chemical picture. Our approach replaces the empirical hard-core model for the $e - H_2$ by a more fundamental quantum statistical treatment. The influence on the equation of state and the composition is small and is concentrated to that region where we have simultaneously the formation of H_2 molecules as well as a large amount of free electrons.

TABLE V. Hard core radius of hydrogen atom and molecule

T , [K]	r_H/a_B , full	r_{H_2}/a_B , full,	r_H/a_B , Ref.[7]	r_{H_2}/a_B , Ref.[7]
10000	6.88	8.65	-	-
11000	6.33	8.25	-	-
12000	5.88	7.90	-	-
13000	5.50	7.58	-	-
14000	5.18	7.30	-	-
15000	4.90	7.05	1.50	1.78
20000	3.91	6.12	1.42	1.70
30000	2.91	5.03	1.30	1.57
50000	2.08	3.96	-	-
60000	1.86	3.65	-	-
70000	1.71	3.41	-	-
80000	1.59	3.21	-	-
90000	1.50	3.05	-	-
100000	1.43	2.91	-	-

ACKNOWLEDGEMENT

This work is supported by the Deutsche Forschungsgesellschaft (DFG) under grant SFB 652 “Strong Correla-

tions and Collective Effects in Radiation Fields: Coulomb Systems, Clusters and Particles”.

-
- [1] R. P. Drake, *High-Energy-Density Physics* (Springer, New York, 2006).
- [2] J. Lewis, *Physics and Chemistry of the Solar Systems* (Elsevier/Academic press, 2004).
- [3] R. Redmer, *Lecture Notes in Physics* **670**, 331 (2005).
- [4] B. Holst, R. Redmer, V. Gryaznov, V. Fortov, and I. Iosilevskiy, *Eur. Phys. J. D* **66**, 104 (2012).
- [5] Y. A. Omarbakiyeva, C. Fortmann, T. S. Ramazanov, and G. Röpke, *Phys. Rev. E* **82**, 026407 (2010).
- [6] E. Beth and G. E. Uhlenbeck, *Physica* **4**, 915 (1937).
- [7] D. Kremp, M. Schlages, and W.-D. Kraeft, *Quantum Statistics of Nonideal Plasmas* (Springer, Berlin, 2005).
- [8] K. Huang, *Statistical Mechanics* (Wiley, New York, 1966).
- [9] W. D. Kraeft, D. Kremp, and et al., *Quantum Statistics of Charged Particle Systems* (Springer, Berlin, 1986).
- [10] F. J. Rogers and A. Nayfonov, *ApJ* **576**, 1064 (2002).
- [11] R. Harcourt, *J. Phys. B* **20**, L617 (1987).
- [12] J. Liu, E. Salumbides, and et al., *J.Chem.Phys.* **130**, 174306 (2009).
- [13] S.Trajmar, D. Truhlar, and J. Rice, *J.Chem.Phys.* **52**, 4502 (1970).
- [14] D. Golden, H. Bandel, and J. Salerno, *Phys. Rev.* **40**, 146 (1966).
- [15] J. Yoon, M.-Y. Song, and et al., *J. Phys. Chem. Ref. Data* **37**, 913 (2008).
- [16] M. Morrison, R. Crompton, and et al., *Aust.J.Phys.* **40**, 239 (1987).
- [17] N.F.Lane, *Rev. Mod. Phys.* **52**, 29 (1980).
- [18] F. Calogero, *Variable Phase Approach to Potential Scattering* (Academic Press, New York, 1967).
- [19] V. V. Babikov, *The Method of Phase Functions in Quantum Mechanics* (Nauka, Moscow, 1988).
- [20] Y. A. Omarbakiyeva, G. Röpke, and T. S. Ramazanov, *Contrib.Plasma Phys.* **49**, 718 (2009).
- [21] R. Redmer, G. Röpke, and R. Zimmermann, *J. Phys. B* **20**, 4069 (1987).
- [22] R. Redmer, *Phys. Rep.* **282**, 35 (1997).
- [23] B. I. Schneider, *Phys.Rev. A* **11**, 1957 (1975).
- [24] N. Levinson, *Kgl. Danske Videnskab Selskab, Mat.-fys. Medd.* **25**, 1 (1949).
- [25] B. Jordan-Thaden and et al., *Phys.Rev.Lett.* **107**, 193003 (2011).
- [26] S. Trajmar, D. Register, and A. Chutjian, *Phys.Rep.* **97**, 219 (1983).
- [27] M. J. Brunger and S. J. Buckman, *Phys.Rep.* **357**, 215 (2002).
- [28] F. Linder and H. Schmidt, *Naturforsch.* **26A**, 1603 (1971).
- [29] J. Muse, H. Silva, and et al., *J.Phys.B* **41**, 095203 (2008).
- [30] K. P. Huber and G.Herzberg, *Molecular Spectra and Molecular structure* **IV** (1979).
- [31] W. Ebeling, A. Foerster, V. Fortov, V.K.Gryaznov, and Y.Polischchuk, *Thermophysical Properties of Hot Dense Plasmas* (Teubner, Stuttgart, 1991).